

1. INTRODUCTION AND PRINCIPAL RESULTS¹

Catherine Mével,² Kathryn M. Gillis,³ and Shipboard Scientific Party⁴

INTRODUCTION

Detailed bathymetric, petrologic, and geophysical surveys along the global mid-ocean-ridge system have greatly modified our view of the stratigraphy of the oceanic crust during the past decade. The simple layer cake model, which requires a continuous elongate magma chamber along an axis, has evolved to a segmented ridge system with a hierarchy of discontinuities that likely reflect mantle dynamics and magma melting processes. Recent models suggest that magma chambers are discontinuous features that are fed intermittently from below at regularly spaced points (e.g., Whitehead et al., 1984; Crane, 1985; MacDonald, 1987). Most models that attempt to predict how the internal stratigraphy of the oceanic crust is influenced by the rate of magma supply, spreading rate, and magmatic vs. amagmatic extension have been developed on the basis of remote geophysical techniques. To test these models, it is important to study not only the basalts erupted on the seafloor, but also plutonic rocks that crystallized within a magma chamber. Because plutonic rocks may show considerable mineralogical and geochemical heterogeneity at a very small scale, it is essential to study continuous sections of the lower crust by deep drilling.

The deep rift valleys of slow-spreading ridges suggest ephemeral magmatism and a low rate of magma supply. Although no seismic evidence exists for the presence of a magma chamber at slow-spreading ridges (Purdy and Detrick, 1986), gravity anomalies along the Mid-Atlantic Ridge (MAR) suggest that magmatic accretion is focused and/or that the crust is thicker at discrete centers along the axis (Lin et al., 1990). These zones of mantle upwelling and associated volcanism occur within individual segments bounded by both transform and nontransform offsets and may explain the chemical discontinuities between segments (Whitehead et al., 1984; Lin et al., 1990; Sempéré et al., 1990). Variation of the ridge morphology within and between individual segments along the MAR reflects the cyclicity of tectonic extension and magmatism (e.g., Karson et al., 1987).

A study of earthquake focal mechanisms at the MAR indicates that brittle failure under extension occurs to depths >10 km, presumably where the lithosphere has had a chance to cool between magmatic episodes (Toomey et al., 1985; Huang and Solomon, 1988). If slow-spread crust is built by small, short-lived magmatic intrusions, it may be predicted that both brittle and ductile deformation occur in Layer 3 while the crust is within the vicinity of a ridge. Because brittle fracturing would enhance hydrothermal flow, the lower crust possibly undergoes significant high-temperature alteration at a ridge. Mylonitic zones within the plutonic sequence of the Bay of Islands ophiolite are interpreted as zones of enhanced permeability that acted as conduits for hydrothermal flow to the lower plutonics (Casey et al., 1990). Seismic reflectors imaged in the lower crust of old Atlantic crust may represent zones of deformation and hydrothermal flow similar to those observed in the Bay of Islands (McCarthy et al., 1988).

These predictions were verified in part when a portion of lower crust was recovered from the slow-spreading (8–12 mm/yr) Southwest Indian Ridge (SWIR) during Leg 118. This unique section of gabbroic rocks sampled at Hole 735B spans a complete range of tholeiitic differentiates, including troctolites, olivine gabbros, gabbro-norites, and oxide-rich olivine gabbros. Sharp lithologic transitions indicate that olivine gabbro was intruded by oxide-bearing gabbro and that the intrusion of the oxide gabbro was localized along deformation zones within near-rigid olivine gabbros. Troctolites intrude both the olivine and oxide gabbros and mark the margins of a second intrusion (Bloemer et al., 1991). The results from Hole 735B confirm the view that the lower crust at slow-spreading ridges is built by small, discrete magmatic intrusions that have complex intrusive relations. The relationship between deformation and the oxide gabbros demonstrates that ductile extension and magmatism have interacted to produce a major modification of the primary magmatic stratigraphy (Dick et al., 1991). The continuity of igneous lithologies across high-temperature ductile deformation zones shows that unrelated igneous units have not been juxtaposed by either ductile or brittle faulting. Ductile shear zones within the gabbroic sequence allowed early penetration of seawater into the lower crust and high-temperature metamorphism (Cannat et al., 1991; Dick et al., 1991; Stakes et al., 1991); the crust remained essentially unaltered away from these major conduits for hydrothermal flow. All these observations suggest that magmatism, tectonism and seawater penetration are strongly interrelated at slow-spreading ridges.

The broad elevated topography of axial summit grabens at fast-spreading ridges is thought to reflect a high rate of magma supply that would require fairly steady-state magma chambers (MacDonald, 1987). Until recently, it has been predicted that large, steady-state magma chambers would produce a thick layered sequence in the lower crust similar to the layered sequences in the Oman Ophiolite and continental layered intrusions (e.g., Pallister and Hopson, 1981). New geophysical data from the East Pacific Rise (EPR) indicate the presence of a thin lens of magma underlain by an extensive crystal mush zone that may extend down to the base of the crust (Detrick et al., 1987; Kent et al., 1990). Gaps in the axial magma chamber reflector along the EPR axis are interpreted as the boundaries of discrete magma chambers, which may account for the chemical diversity seen in the volcanics along axis (Kent et al., 1990). The igneous stratigraphy should vary with the relative size and geometry of the chamber and crystal mush zone, and may or may not show evidence for anhydrous ductile deformation. The evolution of cumulates and the mechanism of melt extraction from long-lived crystal mush zones is not known, but it must differ from crystal mush zones in small, ephemeral magma chambers. For example, a long-lived crystal mush zone may explain why magmas erupted at fast-spreading ridges are generally more evolved than magmas at slow-spreading ridges (Sinton and Detrick, 1992). There should be an inherent ordered igneous stratigraphy in the plutonic sequence with gabbros at high levels being intruded by trondhjemites and ferrogabbros, underlain by a thick layered sequence representing near-steady-state crystal sedimentation on a gradually subsiding floor of a magma chamber. Because the buoyancy of magma would likely concentrate melt toward the top of the magma chamber, ductile deformation would be most evident in the lower plutonics.

¹ Gillis, K., Mével, C., Allan, J., et al., 1993. *Proc. ODP, Init. Repts.*, 147: College Station, TX (Ocean Drilling Program).

² Laboratoire de Pétrologie, CNRS URA736, Université Pierre et Marie Curie, 4 Place Jussieu, 75252 Paris cedex 05, France.

³ Department of Geology and Geophysics, Woods Hole Oceanographic Institution, Woods Hole, MA 02543, U.S.A.

⁴ Shipboard Scientific Party is as given in the list of participants preceding the contents.

Earthquake focal mechanisms for slow- to intermediate-spreading ridges show that the depth of brittle failure decreases with increasing spreading rate (Huang and Solomon, 1988). These data predict that brittle faulting at fast-spreading ridges would be restricted to the upper few kilometers of the crust, suggesting that the brittle-ductile transition occurs at or near the top of the magma chamber (Huang and Solomon, 1988). The brittle zone probably does not extend down into the lower crust until the crystal mush zone starts to solidify and crack because of thermal contraction. Because the absence of ductile deformation should preclude the early penetration of seawater into the solidified lower crust, high-temperature metamorphism may not be a significant process beneath fast-spreading ridges, producing a pattern of hydrothermal alteration in the lower crust that is different from slow-spreading ridges (Mével and Cannat, 1991).

Another major issue of lithosphere creation and evolution at mid-ocean ridges is the understanding of processes occurring in the upper mantle and the crust-mantle transition. In ophiolites, a somewhat thick transition zone is composed of alternating dunite and harzburgite tectonites, with the proportion of harzburgite increasing downward (see review in Nicolas, 1989). The internal stratigraphy and composition of dunites/harzburgites reflect the processes of melt migration and extraction critical to understanding the evolution of mid-ocean-ridge basalt. The extent to which these processes occur beneath ocean ridges is unknown, although essential, in modeling the generation of ridge basalts.

The nature of the seismically defined Moho beneath ridges is still being debated. Although the Moho is generally viewed as a simple igneous stratigraphic boundary, investigations of ophiolites demonstrate that it may be either a wide transition zone or a tectonic contact. A well-preserved, intact igneous Moho is most likely to occur beneath fast-spreading ridges, as extension accompanying divergence of the plates may be simply accommodated by flow in a crystal mush zone and partially molten mantle.

Processes controlling seawater penetration in the mantle are still poorly understood; understanding the chemical effects of serpentinization is important to assess its impact on the chemical budget of the oceans. The serpentinization process also decreases the density and velocity of the mantle and, thus, may influence the physical properties of mantle. Serpentinization also is responsible for the formation of secondary magnetite, which may allow mantle rocks to contribute significantly to the formation of magnetic anomalies.

To address these important questions concerning crustal and upper mantle processes one site in the lower crust and one site in the shallow mantle were drilled at Hess Deep during Leg 147.

Geologic and Tectonic Setting

Hess Deep is the deepest part of a westward-propagating oceanic rift valley that is opening up the eastern flank of the equatorial EPR in advance of the westward-propagating Cocos-Nazca spreading center (Lonsdale, 1988) (Fig. 1). The western end of the rift valley is 30 km from the EPR axis, where approximately 0.5-Ma EPR crust is broken by two 5-km-wide east-west grabens, which join a few kilometers farther east. As the rift valley is traced eastward, it broadens to 20 km and deepens to >5400 m; its uplifted shoulders rise to depths less than 2200 m. Approximately 70 km east of the EPR axis, the Cocos-Nazca spreading center begins to build a volcanic ridge in the rift valley, and the rift escarpments are locally uplifted an additional 500 m at narrow horsts. Farther east, the wedge of newly accreted crust formed by north-south spreading expands to a mature, medium-rate (50 mm/yr total) spreading center, and the rift escarpments become the "rough-smooth boundary" of the Galapagos gore.

The Hess Deep rift valley is propagating into a random part of the EPR at a rate that matches the 65 km/m.y. half rate of EPR spreading (Lonsdale, 1988). Before ~1.3 Ma, the Hess Deep area was a steady-state triple junction between the Cocos-Nazca ridge and the EPR. A change in the spreading direction of the EPR at ~1.3 Ma corresponds

with the initiation of the Galapagos microplate, making the Hess Deep rift valley the Cocos-Galapagos rather than the Cocos-Nazca boundary. Magnetic isochrons on either side of this boundary are offset across the rift valley, with the 1 Ma isochron being further west on the northern than southern rift margin. The orientation of abyssal hill lineations from the EPR eastward to Hess Deep, both along the northern scarp and within the microplate, deviates significantly from the EPR trend. A recent SeaBeam survey on the conjugate flank of the EPR shows similar variation, suggesting that discrete blocks of crust were rotated during transport off-axis (P. Lonsdale, pers. comm., 1992). An interpretation of these data suggests that the overlapping spreading center (OSC) currently centered at 2°20'N has alternated between northern and southern propagation since the change in spreading direction at ~1.3 Ma. This would produce a complex juxtaposition of crustal blocks generated at different segments of the EPR. For example, a crustal section generated at the western flank of the EPR may be captured during southward propagation and transported off-axis on the eastern flank. This model accounts for the offset in the magnetic isochrons and predicts that the crust exposed at Hess Deep is composed of crustal blocks generated at different margins of the EPR.

The fault scarps that bound the rift valley are seismically active (Neprochnov et al., 1980) and are exposing 0.5- to 1.0-Ma crust. Rocks observed on these scarps appear to have been freshly exposed and are not encrusted with manganese oxides. The rift valley is asymmetric, with the Hess Deep ridge axis occurring closer to the southern than the northern wall. The southern wall rises continuously in large steps to a crest of 2200 m depth, approximately 7 km south of the deep. The EPR plateau is fairly flat, and abyssal-hill lineations intersect the scarp. Abyssal-hill lineations within the northern scarp generally extend up to the scarp except in the area of a rift-shoulder horst, where a crustal block has been rotated. Soviet multichannel reflection profiling along the EPR flanks indicates that seismic Layers 2A (lava sequence) and 2B (dike complex) are of normal thickness (about 2 km) and that Layer 3 (gabbroic complex) may be somewhat thinner than usual (3–3.5 km) (Zonenshain et al., 1980). A major intrarift ridge occurs between Hess Deep and the northern scarp and extends eastward, overlapping the western end of the Cocos-Nazca ridge (Fig. 2).

The geology of the Hess Deep region was investigated during two submersible cruises: in 1988, the floor and walls of the rift valley were studied with the *Nautilé* during a series of 22 dives (Francheteau et al., 1990; Francheteau et al., 1992), and in 1989, the rift valley walls were investigated with the *Alvin* in a series of 11 dives (P. Lonsdale, unpubl. data; Karson et al., 1992). The following is a summary of the results of these field programs.

Volcanics, sheeted dikes, and, locally, gabbros crop out along the scarps that bound the Hess Deep rift valley. A talus ramp intersects the scarps within the sheeted-dike complex that is approximately 1200 m thick. Dikes are generally subvertical and strike north-south, parallel to the EPR fabric. Gabbros underlie the sheeted dikes within a rift shoulder horst along the northern scarp. In this region, the dikes are locally rotated. Typically, a 100- to 300-m-thick layer of pillow lavas is separated from the sheeted dikes by an intermediate zone of variable thickness (50–500 m), consisting of a mixture of extrusives and intrusives, including thick horizontal layers that may represent sills.

A complete, albeit dismembered, crustal section of the EPR, including volcanics, sheeted dikes, gabbros, and peridotites, is exposed on the floor of the Hess Deep rift valley and the intrarift ridge. This area was investigated along two north-south trending transects that were centered at the western (3040 m) and eastern (2900 m) summits of the intrarift ridge (Fig. 2; Francheteau et al., 1990). Along the western transect, the slope that rises southward from the axis of Hess Deep averages 45° and is covered with basaltic and diabasic rubble. A gentle, 15°–20° slope, stepped with secondary high-angle faults, extends north of Hess Deep for 5–6 km. Lower crustal rocks with rare dunites crop out in ledges that dip into the lower slope from 5400- to 4500-m depth, and semi-horizontal ledges of dolerite occur in a mainly sedimented terrain between 4500 and 4000 m. A change in slope at 4000 m marks

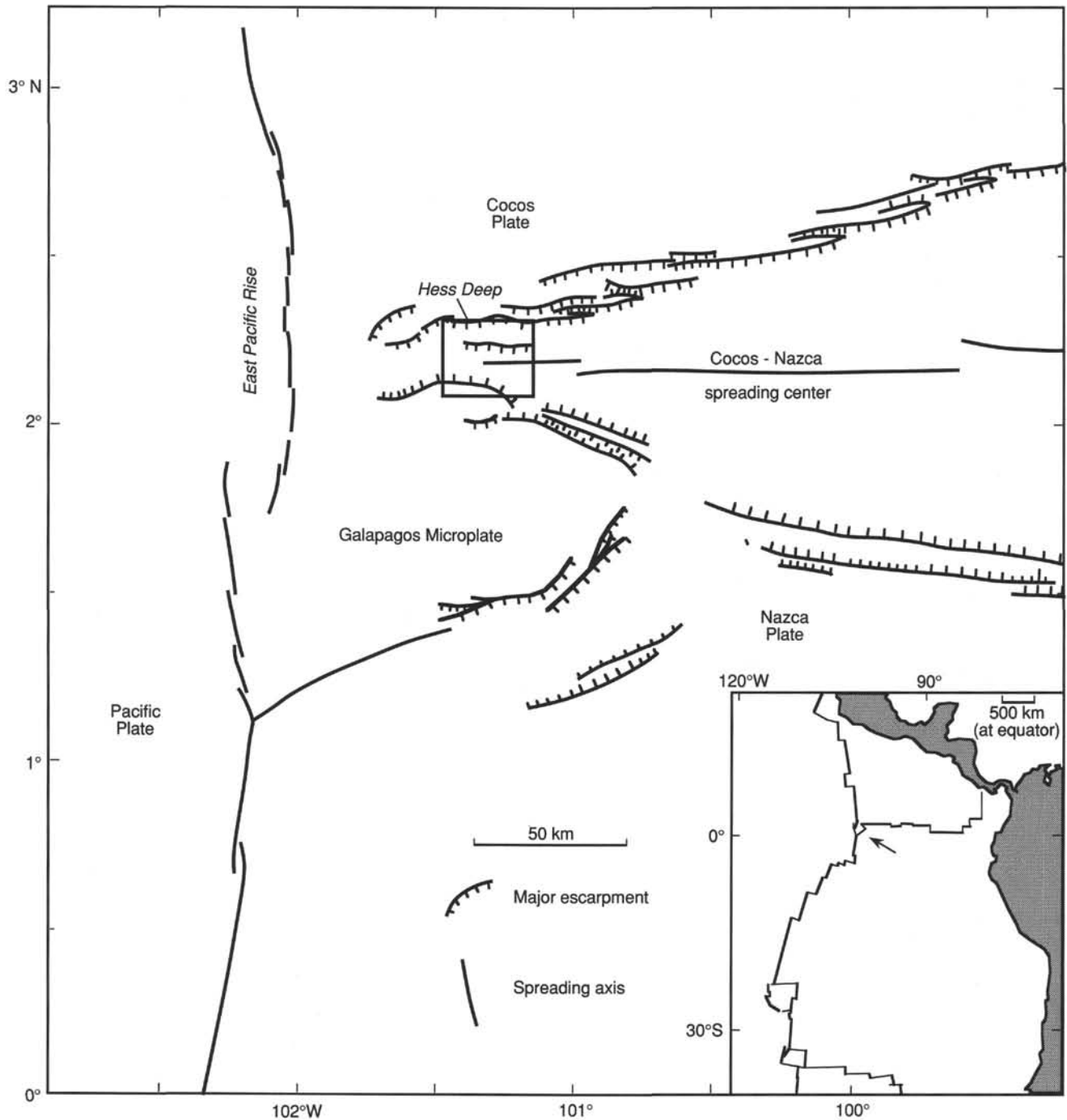


Figure 1. Location of Hess Deep at the western end of the propagating Cocos-Nazca spreading axis (modified from Lonsdale, 1988).

the southern edge of the east-west-trending intrarift ridge, which culminates at 2900 meters below sea level (mbsl). In this area, gabbros crop out along the southern and northern slopes with an isolated basalt outcrop at the ridge's crest. Along the eastern transect, north of the tip of the Cocos-Nazca ridge, plutonic and ultramafic rocks crop out between 4500- and 3500-m depth along a gentle slope that is locally $\leq 10^\circ$. Cr-spinel-bearing dunites and harzburgites were sampled from subhorizontal ledges that dip to the north. Pillow lavas and dikes form the crest of the ridge at the eastern summit, and low-temperature hydrothermal activity was observed. In-situ north-south trending dikes crop out on the northern slope of this summit. Gabbros have been recovered by well-positioned dredges between these two transects (Fig. 2). Along both transects, the slope south of the intrarift ridge and

north of Hess Deep and the Cocos-Nazca rift tip has undergone significant mass wasting and talus accumulation.

The distribution of rock types along the eastern and western transects shows that the structure of Hess Deep is complex. There is no lateral continuity in rock type between the two transects, and the geology in between is unknown. Cumulate gabbros occur at deeper depths along the western transect than do harzburgites along the eastern one. Moreover, observations suggest that the western end of the intrarift ridge is composed of a massive block of gabbros, whereas the eastern end consists of upper crustal rocks, dolerites, and basalts.

Two alternative rifting models have been proposed for the Hess Deep rift valley (Francheteau et al., 1990). One emphasizes the vertical movement of mantle horsts or serpentine diapirs to expose mantle

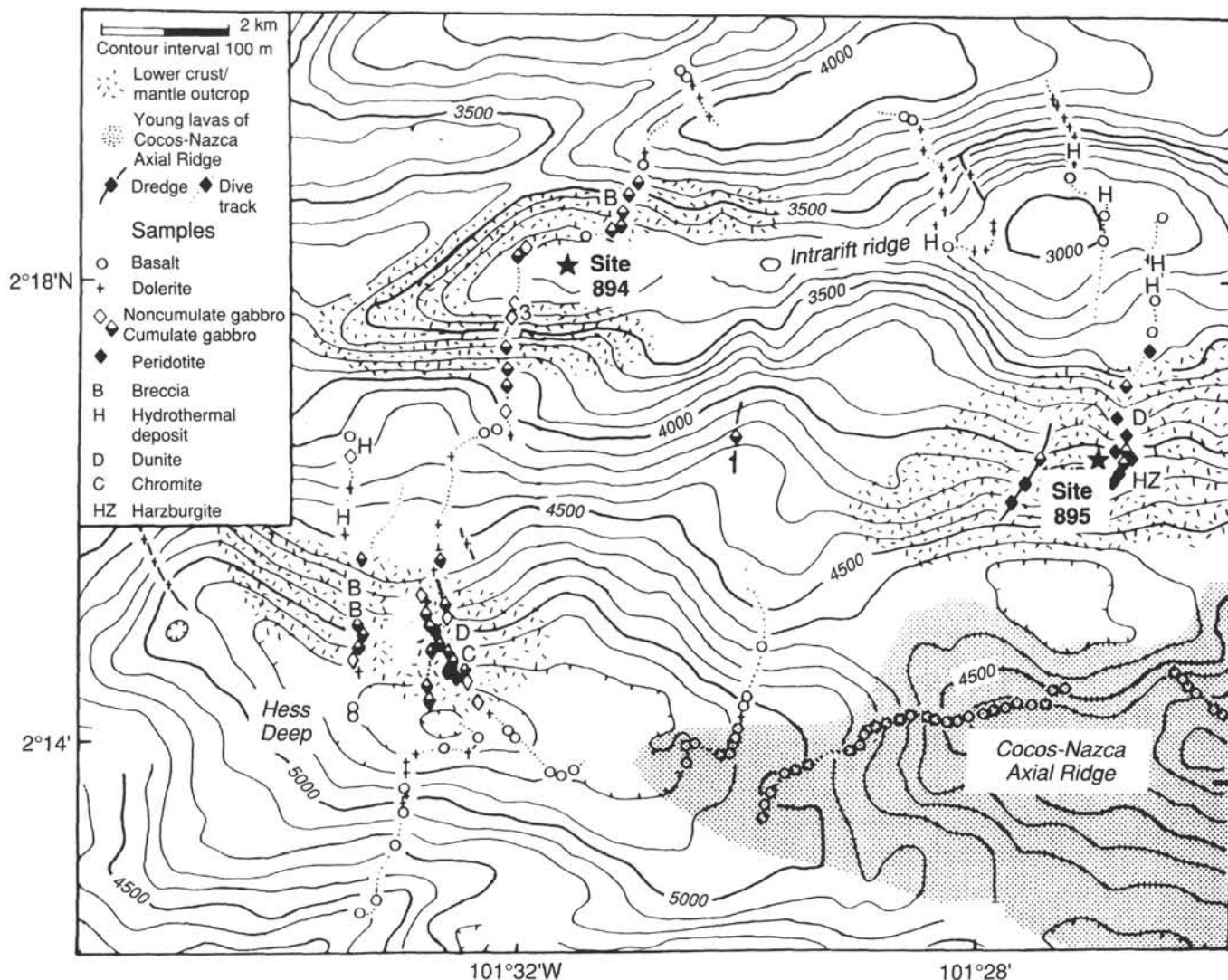


Figure 2. Geologic and bathymetric map of the Hess Deep rift valley. Geology is based upon the *Nautilie* dive series and the dredge results from the *SONNE* and *Atlantis II* (modified from Francheteau et al., 1990). Stars indicate the locations of drill Sites 894 and 895.

rocks. The other postulates rupture of the lithosphere by low-angle detachment faults similar to those mapped and imaged at rifting sites in continental lithosphere and recently postulated for the regenerating axial rift valleys of slow-spreading ridges. Both models are compatible with the observed bathymetry and outcrop distribution (Fig. 3). However, preliminary interpretation of on-bottom gravity and seismic data collected across the intrarift ridge indicates that the ridge is composed of high-density and high-velocity material (L. Dorman and J. Hildebrand, pers. comm., 1992; Wiggins et al., 1992). These new data suggest that the intrarift ridge is a block of dense lower crustal and mantle rocks, supporting the latter model.

Sedimentary Sequence

Little is known about the sedimentary cover of the Hess Deep rift valley. Compared with sedimentation rates in the area (see "Sediments" section, "Site 894" chapter, this volume), sediment thicknesses along the intrarift ridge appear to be thin (2–4 m). The thickest accumulation of sediment (20 m) was imaged by 3.5 kHz echosounder profiles during the *SONNE 60* cruise within the lower part of the deep (Blum, 1991). *Nautilie* dives revealed that a sediment blanket covers most of the

seafloor, except along steep slopes, and seems to have been deposited by turbiditic currents (Francheteau et al., 1990; Blum, 1991). Recovered sediments are primarily pelagic ooze, hydrothermal component such as pyrrhotite, pyrite, and silica (Rudnick, 1976; Murdmaa and Rozanova, 1976), and variably altered igneous lithic fragments. Hydrothermal serpentine was recovered in a sediment core (Schmitz et al., 1982) from the floor of Hess Deep and is interpreted as being derived from mass wasting from the southern flank of the intrarift ridge.

Extrusive Rocks

Basalts were recovered from the scarps of the rift valley, from the tip of the Cocos-Nazca propagator, along the slope south of the intrarift ridge and north of the deep between 4500 and 4000 m, and as isolated pods on top of the intrarift ridge. Volcanics from the rift scarps and valley floor are moderately plagioclase- and olivine-phyric, whereas those from the Cocos-Nazca spreading center are highly plagioclase-phyric. Basalts from the rift floor fall within the compositional range of EPR (e.g., at 12°52'N, Hekinian et al., 1989) and Cocos-Nazca basalts (Blum, 1991), and their K/Ti ratios and Mg#s indicate depleted, transitional, and undepleted groups (Hekinian et al., 1993). The intrarift

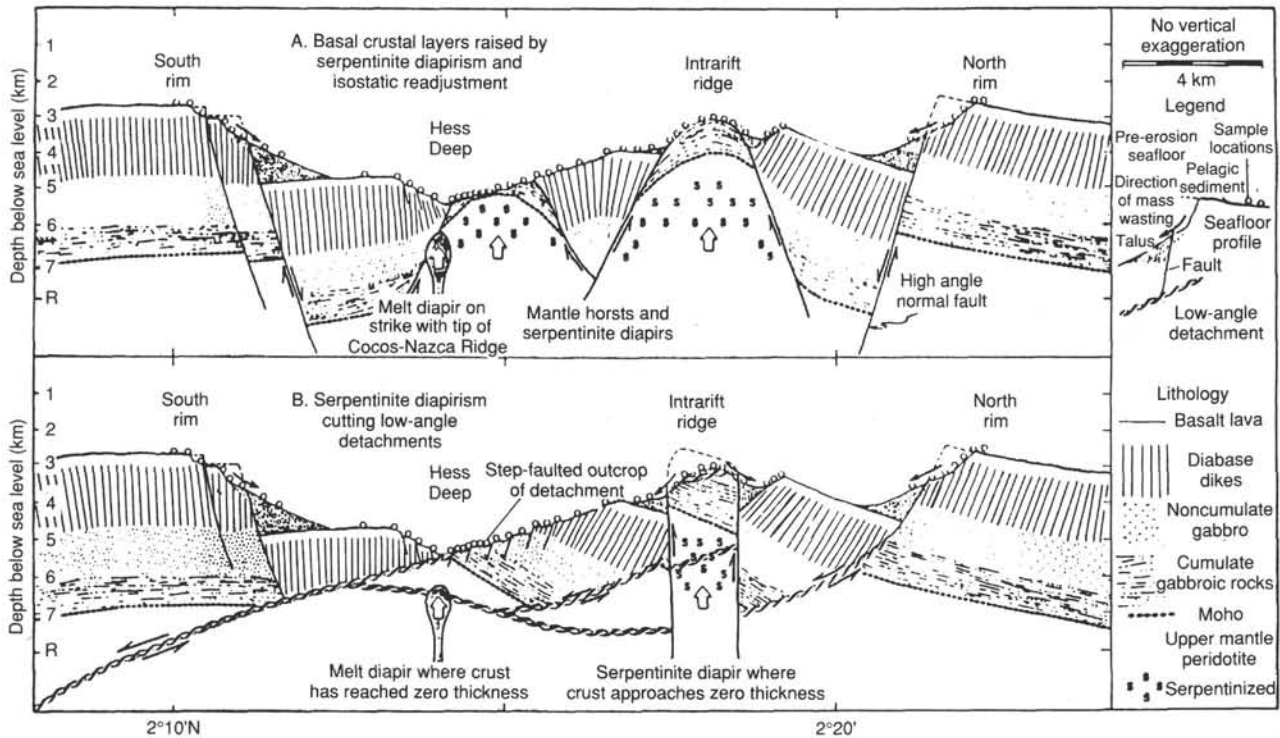


Figure 3. Interpretive cross sections depicting two models that account for the surficial geology and bathymetry of the Hess Deep rift valley (Francheteau et al., 1990).

ridge basalts are consistently depleted in titanium (Blum, 1991), however, relative to the Cocos-Nazca basalts and EPR basalts recovered from the Hess Deep scarps (J. Natland, pers. comm. 1992).

Plutonic and Ultramafic Rocks

Plutonic and ultramafic rocks were recovered from the rift valley floor and the intrarift ridge, as well as the northern scarp. The ultramafic rocks consist of harzburgites and dunites (Hekinian et al., 1993). Although largely serpentized (the freshest sample contains 60% serpentine), harzburgites still exhibit porphyroclastic textures that are typical of mantle rocks, and a few samples are impregnated by a wehrlitic melt (Girardeau and Francheteau, 1993). The dunites are even more serpentized and may contain some amoeboid plagioclase that is interpreted to be the result of impregnation by a basaltic melt. These rocks are thought to correspond to the transition zone between the base of the gabbros and the mantle.

Plutonic rocks include olivine gabbro cumulates, gabbro cumulates (lacking olivine and chromite) and noncumulate olivine gabbros, gabbroic rocks, and gabbros. Mineralogical (Hekinian et al., 1993) and geochemical (Blum, 1991) data show that cumulate gabbros are more abundant on the slope south of the intrarift ridge, and that the most magnesian gabbros lie at the greatest depths, suggesting formation within the lower levels of a magma chamber. Many of the gabbros have been metamorphosed, and amphibolitization and albitization may be extensive enough to obliterate the primary mineralogy. Abundant calc-silicates (prehnite, zeolites, epidote) characterize the metamorphism of olivine gabbro cumulates, which are partially or completely rodingitized. Stable isotope ratios suggest that interaction with seawater occurred mostly under greenschist facies conditions (Agrinier et al., unpubl. data). Cataclastic mylonites also have been recovered at several depths on both the southern and northern slopes of the intrarift ridge.

PRINCIPAL RESULTS

Introduction

During Leg 147, the evolution of crustal processes at a fast-spreading ridge was investigated at two sites within the Cocos-Nazca rift valley at Hess Deep (Fig. 4). A sequence of high-level gabbroic rocks, interpreted to have formed along the roof of an axial magma chamber, was recovered at Site 894, located at the crest of the western end of an intrarift ridge. At Site 895, located 9 km southeast of Site 894, a

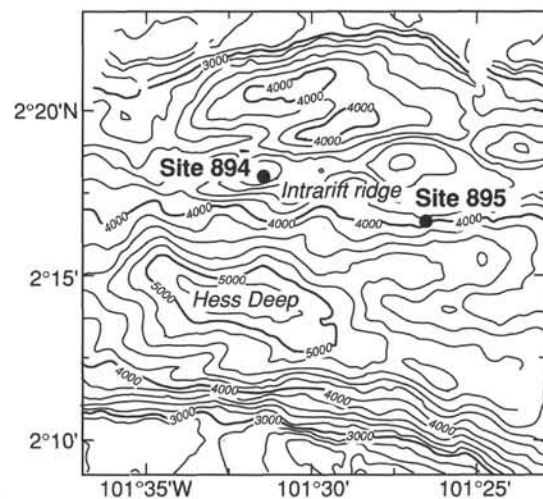


Figure 4. Location of Sites 894 and 895 at Hess Deep. Bathymetric contours from SONNE data (Cruise report, SONNE 60, 12 March 1988–2 January 1989).

sequence of mafic (troctolites, olivine gabbros, gabbros, and basaltic dikes) and ultramafic (dunites, harzburgites) rocks was recovered in the vicinity of the transition zone between the lower magmatic crust and upper residual mantle.

Site 894

Seven holes were drilled at Site 894 within a 215-m (east-west) by 280-m (north-south) area at the crest of the intrarift ridge. Shallow holes were drilled on the flat-lying, slightly sedimented summit of the ridge (Holes 894A, 894D, and 894E) and on ledges close to the southern edge of the summit (Holes 894B, 894C, and 894F) to locate appropriate rock types and evaluate drilling conditions. Drilling at Hole 894F penetrated 25.7 m and recovered 1.8 m of cataclastically deformed gabbro, olivine gabbro, and aphyric basalt. As conditions were appropriate for placement of a hard-rock guide base at this location, Hole 894G was initiated 10 m west of Hole 894F. In Hole 894G, the upper 18.6 m was drilled but not cored, as an equivalent section was recovered from Hole 894F. Thus, Holes 894F and 894G are considered contiguous sections. Drilling at Hole 894G penetrated 154.5 mbsf and recovered 45.78 m of core.

Site 895

Six holes were drilled at Site 895 at three different locations along the southern slope of the intrarift ridge. The rationale for emplacing the holes was to determine the lateral variability of the shallow mantle. Ultramafic rocks and minor quantities of gabbroic rocks and basaltic dikes were recovered. Recovery at Hole 895A consisted of 1.78 m of highly perturbed sediments that included clasts of serpentinized peridotite, gabbro, and basalt. Holes 895A, 895B, 895C, and 895D are located within 20 m, at a depth of 3821 mbsf. Holes 895A and 895B were abandoned after less than 20 m of coring. At Holes 895C and 895D, drilling penetrated 37.9 m and 93.7 m and recovered 5.79 m and 19.08 m, respectively. Hole 895E is located upslope, 300 m north of Hole 895D, at a depth of 3752.5 mbsf. Drilling penetrated 87.9 m, and 37.47 m was recovered. Hole 895F is located upslope about 200 m north of Hole 895E, at 3792.5 mbsf. A total of 26.2 m was penetrated and 1.98 m was recovered. However, conditions indicated that Hole 895F probably cored through a rubble pile.

Petrology and Geochemistry of the Gabbroic Rocks from Site 894

The igneous lithologies recovered at Site 894, in order of their abundance, are gabbro, olivine gabbro, olivine gabbro, oxide gabbro, and basalt (see Table 6 in the "Site 894" chapter, this volume). At Holes 894F and 894G, 13 lithologic units were recognized on the basis of mineralogy, texture, and grain size (see Figs. 5 and 6 in the "Site 894" chapter). Variably deformed gabbro and olivine gabbro compose Hole 894F and the upper part of Hole 894G. Gabbro first appears at 40 mbsf and becomes the major lithology throughout the remainder of the hole. Gabbro and olivine gabbro intervals recur in minor quantities intermittently downhole. Although Fe-Ti oxide minerals are present within most plutonic lithologies, oxide-rich zones (with >5% Fe-Ti oxides) rarely occur in gabbros. The lithologies at Holes 894F and 894G exhibit a significant range in texture and grain size downhole (see Figs. 5 and 6 and the "Igneous Petrography of Holes 894F and 894G" section in the "Site 894" chapter). The most common textures are poikilitic and equigranular hypidiomorphic. Poikilitic texture typically involves orthopyroxene oikocrysts and, to a lesser degree, clinopyroxene. Changes in texture on a thin section and hand specimen scale are very common, and patches of equigranular gabbro occur within poikilitic gabbro in several sections of core. Coarse-grained to pegmatitic patches in gabbro and gabbro locally contain zircon and apatite, in association with primary oxides and amphibole. The presence of

primary, vapor-dominated fluid inclusions in apatite suggests that these accessory phases may have a deuteric origin.

Centimeter-thick veins of medium- to coarse-grained gabbro locally cut poikilitic rocks, which locally exhibit a magmatic lineation of plagioclase. At a number of locations, large sections of the core alternate between poikilitic and equigranular textures. These variations may correspond to layering or, more likely, represent large patches of one textural type within the other. Equigranular gabbro increases in abundance and becomes coarser grained toward the lower half of the recovered core.

Magmatic penetrative fabrics, defined by the alignment of tabular plagioclase crystals, are intermittently distributed below 50 mbsf and are most prevalent between 100 to 120 mbsf. This foliation is steeply dipping, with a mean dip of 75° (standard deviation of 13°). The average trend of the foliation, restored with reference to core paleomagnetic data, is close to north-south (i.e., near parallel to the strike of the East Pacific Rise spreading axis). The magmatic foliation is best developed in the fine-grained gabbros, but a weak-to-moderate fabric also occurs in some of the coarser-grained gabbros. The transition from unfoliated poikilitic gabbros to foliated rocks is gradational on both macroscopic and microscopic scales. Where finer-grained gabbro and coarser-grained gabbro are in contact, the magmatic foliation in the former is slightly oblique to, and cut by, the igneous contact, which typically has a steeper trend. Where magmatic foliations are developed in medium-grained poikilitic gabbro, orthopyroxene is either a minor phase or is absent from the rock. This suggests that development of a foliation involves not only an alignment of tabular plagioclase, but also the disappearance of late crystallizing orthopyroxene.

The mineralogy and textures of the plutonic lithologies recovered at Site 894 suggest the fractionation series olivine gabbro, olivine gabbro, gabbro, and oxide gabbro. This sequence represents the crystallization order: (1) olivine-plagioclase-clinopyroxene, (2) orthopyroxene- (olivine/melt reaction) plagioclase-clinopyroxene, and (3) orthopyroxene-plagioclase-clinopyroxene co-crystallization, with the development of accessory oxide minerals, zircon and apatite. It is reflected in a progressive decrease in the abundance of Cr with depth. These characteristics indicate that the rocks crystallized from tholeiitic magma that became progressively more evolved downhole. The presence of several olivine gabbro intervals intermittently downhole may reflect smaller-scale fluctuations in magma compositions that may be related to episodic influx of more primitive magma within the axial magma chamber. These lithologic and geochemical trends represent a sequence of high-level gabbros that probably crystallized from the roof of a magma chamber downward. The lack of well-developed modal layering, the variation in texture and grain size, and the presence of evolved rock types are comparable to the upper plutonic sections of many ophiolites.

The occurrence of coarse-grained to pegmatitic patches of gabbro adjacent to foliated, medium-grained rocks that lack interstitial orthopyroxene suggests that melt segregations were locally filter-pressed from the surrounding foliated host. Moreover, the occurrence of coarse-grained gabbro as dikelets or vein-like patches that slightly postdate the main foliated fine-grained gabbro suggests that accumulation and flow of interstitial melts played an important role at this level in the crust.

The gabbroic rocks recovered at Site 894 are variably altered to lower amphibolite to zeolite facies mineral assemblages (see Table 8 in the "Site 894" chapter, this volume). Overprinting of higher-temperature secondary minerals by lower-temperature phases is common, and the intensity of alteration downhole is heterogeneous. At least 80% of the gabbros recovered at Site 894 are affected by 20%–50% background replacement of primary minerals, with more altered local intervals displaying 50%–100% replacement. Samples exhibiting less than 15% modal alteration are extremely rare.

Several generations of veins crosscut the gabbroic rocks. The earliest veins include micron-size amphibole along grain boundaries

between relict igneous minerals and dense arrays of linear fluid inclusion trails. These microscopic veins appear to be conduits that facilitated the flow of fluids that were responsible for incipient static metamorphism. Three types of macroscopic veins that post-date the microscopic veins were distinguished on the basis of mineral assemblages. The earliest are filled primarily by green amphibole, with rare pale brown amphibole, chlorite, and sphene. Fractures filled by chlorite + prehnite + actinolite + epidote postdate the amphibole veins and are typically associated with strong wall-rock alteration to sodic plagioclase, actinolite, chlorite, sphene, and local epidote and prehnite. These chlorite veins systematically have true dips of 40°–60° and a west-northwest strike (restored with respect to stable magnetic vector data). The youngest veins are filled by combinations of chlorite, smectite, zeolites, and calcite. No consistent orientation was observed for the earliest and latest vein types.

Vein density, or the number of veins per unit length, varied from 0 to 0.44 cm⁻¹ in Hole 894G with a mean of 0.21 cm⁻¹. Vein densities are 0.29 cm⁻¹ in the upper 10 m, and decrease sharply to an average of 0.22 cm⁻¹ in the remainder of the hole. These values are significantly higher than in plutonic rocks in the Semail Ophiolite (0.01 cm⁻¹; Nehlig and Juteau, 1988) or Skaergaard Intrusion (0.06 cm⁻¹; Bird et al., 1986).

Deformation of Site 894 gabbros was accommodated entirely by brittle processes, and the rocks show no evidence for solid-state penetrative deformation. Cataclastic shear zones are restricted to the upper portions of Holes 894C, 894F, and 894G, whereas minor distributed cataclasis (i.e., fault brecciation) is found locally throughout Hole 894G. Cataclastic shear zones vary in their texture, ranging from homogeneously distributed zones of cataclasis through development of protocataclasis to cataclasis and ultracataclasis, with increasing strain. Veining and pervasive alteration is typically associated with cataclastic shear zones. The alteration mineralogy of these shear zones suggests that temperatures were less than 400°C, which excludes the possibility of dynamic recrystallization.

Petrography and Geochemistry of the Basaltic Rocks from Site 894

Basaltic rocks were recovered in Holes 894D, 894E, 894F, and 894G. Fine-grained, aphyric basalts from Holes 894D and 894E are interpreted as volcanics similar to those observed locally within the Hess Deep rift valley during the *Nautila* dive program (Francheteau et al., 1990). The origin of these extrusive rocks is not well constrained but is thought to be related to the opening of Hess Deep.

One aphyric basaltic dike was recovered in Hole 894F, and two porphyritic basaltic dikes were recovered in Hole 894G. Both porphyritic dikes are plagioclase, olivine, and Cr-spinel phyrlic and have high bulk rock (Mg/Mg + Fe), high Cr and Ni contents, and low Zr and Y contents. Their compositions overlap those of the most primitive of Cocos-Nazca volcanics (Blum, 1991) and are more primitive than volcanics erupted along the East Pacific Rise (e.g., Langmuir et al., 1986).

Alteration of the basaltic dikes is variable and heterogeneous, ranging from 10% to 85% replacement of primary minerals by greenschist facies mineral assemblages. Two generations of veins cut across the basaltic dikes: an early chlorite + actinolite and later chlorite + clays (dominantly smectites) ± zeolites. The most intense alteration is associated with chilled margins bounding gabbroic rocks and adjacent to vein networks.

Petrography of Site 895 Igneous Rocks

Serpentinized harzburgites and dunites are by far the most abundant rock type recovered at Site 895, although minor quantities of mafic rocks (troctolites, olivine gabbro, gabbro) and basaltic dikes also are present. The proportion of these four rock types varies between Holes 895D and 895E, the holes with the greatest depth penetration and core

recovery. Gabbroic rocks and dunites are most abundant in Hole 895E (see Table 2 of the "Site 895" chapter, this volume).

In general, harzburgites are relatively poor in orthopyroxene (less than 15% by mode) and often exhibit a gradational change to dunite. Small dunitic patches commonly occur in harzburgite, as do patches of porphyroclastic harzburgite in dunite. Clinopyroxene is characteristically sparsely present (typically less than 1% by mode, but rarely up to 3%). It is locally found as exsolution lamellae within primary orthopyroxene or attached to orthopyroxene, either around the rims of porphyroclasts or recrystallized in a matrix of orthopyroxene neoblasts. Vermiform intergrowths of clinopyroxene with fine-grained spinel also occur. The harzburgites also contain dark red spinel.

Dunite is composed of olivine and chromian spinel (1% to 2% by mode) with or without pyroxene (less than 10% by mode) that is typically interstitial to olivine. Dunites may appear partially impregnated by melts in some intervals. This is particularly spectacular in Hole 895C where plagioclase is interstitial to clusters of olivine grains and may be intergrown with interstitial clinopyroxene, and spinel is locally present. In most cases, coarse-grained gabbroic and troctolitic rocks are intercalated with serpentinized dunite and harzburgite, and contact relationships are scarce. Gradational transitions between troctolite and troctolitic gabbro occur, and gabbros locally crosscut troctolites in a few pieces. Gabbroic rocks are more abundant in Hole 895E, which contains the greatest proportion of dunite among the holes drilled at Site 895.

Despite pervasive serpentinization, harzburgites retain porphyroclastic textures. Spinel shape fabric in both dunites and harzburgites defines a foliation attributed to high-temperature solid-state flow. In Holes 895C, 895D, and 895E, the spinel foliation seems to show an increasing amount of dip with depth. In dunite and troctolite, traces of plastic deformation of olivine are observed in thin section.

The rock types recovered at Site 895 are extensively altered (see Table 6 and the "Metamorphism" section in the "Site 895" chapter, this volume). Static metamorphism is the dominant process controlling alteration. Alteration of the harzburgites varies from 50% to 80% in Holes 895A through D and is commonly greater than 90% in Hole 895E. As a rule, dunites are more altered than harzburgites. Alteration is dominated by the replacement of olivine by serpentine associated with lesser amounts of bastite, talc, magnetite, chlorite, brucite, clay, and trace antigorite. Troctolitic and gabbroic rocks are moderately to pervasively altered and commonly exhibit well-developed coronitic replacement of olivine and plagioclase. Secondary minerals include chrysotile, tremolite, and magnetite after olivine, and prehnite, chlorite, zeolite ± hydrogrossular after plagioclase. This last association suggests an incipient rodingitization. In the most pervasively altered samples, tremolitic patches bounded by fine rims of clinopyroxene and chlorite are common.

In the ultramafic rocks, multiple vein generations crosscut the pervasive background mesh serpentine texture. Early veins are filled with tremolite, Mg-chlorite with minor antigorite(?), and magnetite. They are crosscut by several generations of veins filled with chrysotile, magnetite, brucite, clays, and zeolites. Fibrous aragonite + chrysotile form the latest generation of veins. Veins show a variety of orientations, but no relationship exists with differing vein assemblages. Vein dips are widely scattered, whether plotted relative to the axis of the borehole or corrected assuming the inclination of the stable magnetization to be zero.

Veins in gabbroic rocks are commonly monomineralic, thin and discontinuous, and are filled with amphibole, talc, chlorite, prehnite, and zeolite. Rare brown amphibole forms crosscutting veinlets in basaltic samples.

The pervasive metamorphism and associated vein formation in ultramafic and mafic rocks recovered from Site 895 reflect extensive interaction with seawater-derived fluids. In ultramafic rocks, the temperature of interaction is difficult to estimate, although the presence of tremolite and chlorite suggests that it started under greenschist

or lower amphibolite facies conditions. However, the temperature at which the bulk of the serpentinization occurred is unknown. The strong control of primary mineralogy on the spatial distribution of secondary minerals in the serpentinized peridotites suggests that fluid-rock interaction was rock-dominated. The close association of local calcium-metasomatized gabbroic rocks with the peridotites may reflect migration of calcium-rich fluids generated during serpentinization of the peridotites (incipient rodigitization).

Paleomagnetic Results from Sites 894 and 895

Previous studies of the magnetic properties of the lower oceanic crust and mantle have been based primarily on samples dredged or drilled at slow-spreading ridges. The cores recovered at both Sites 894 and 895 are important because they represent lower crust and mantle formed at a fast-spreading center.

Natural remanent magnetization (NRM) intensities from both sites show a wide range of magnitude (Fig. 5). This large variation reflects the lithologic variety, with dunites having a higher NRM intensity than harzburgites and gabbros. The high average NRM intensities of both gabbroic and ultramafic rocks (2.0 and 3.0 A/m, respectively) are consistent with previously reported values. Although the high magnetizations suggest that gabbros and serpentinized peridotites may contribute to seafloor magnetic anomalies, the formation of magnetite as an alteration product raises questions regarding the timing of the acquisition of remanent magnetization.

Magnetic susceptibility varies between 0.0006 and 0.06 SI unit in Site 894 gabbros and from 0.0003 to 0.13 SI unit at Site 895. As with NRM intensities, peridotites, at 0.045, have a higher mean (dunites being higher than harzburgites) than 894 gabbro samples, which average 0.016. Again, the values are consistent with values previously reported.

The Koenigsberger ratio (Q) compares the relative importance of the remanent magnetization to the magnetization induced in the formation by the Earth's magnetic field. Except for four peridotite samples, Q values for both sites are greater than 1, indicating that remanent magnetization is predominant in total in-situ magnetization. Higher Q ratios from Hole 894G gabbros than from the Site 895 peridotites suggests that coarser-grained magnetites are the remanence carriers for peridotites.

Both alternating field (AF) and thermal demagnetization were performed on selected minicores from both sites. The NRM of gabbros from Site 894 was generally quite resistant to thermal and AF demagnetization, except for a small number of highly altered samples. By contrast, serpentinized peridotites from Site 895 were easily demagnetized. For 894 gabbros, the sharp decrease in magnetization at about 550°C in the thermal demagnetization curves suggests that the NRM is carried by a single magnetic phase, which is likely magnetite. The thermal demagnetization curves also suggest that the peridotites have a larger magnetic grain-size distribution than do the gabbros. In both mafic and ultramafic rocks, magnetite occurs as a secondary mineral, intergrown with actinolite or chlorite in the gabbroic rocks, and with serpentine in the peridotites. Only in a few oxide gabbro samples may magnetite be present as a primary phase. This suggests that at both sites most of the NRM was acquired as a result of alteration.

Subsequent to demagnetization, individual components of magnetization were identified for minicores from both sites. At Site 894, more than half of the samples have two components of magnetization, and four samples have three. Stable inclination values for Hole 894G are consistent and show a general steepening with depth, from 30° to 50°. The steepening with depth could be related to hole deviation (see "Operations" section, "Site 894" chapter, this volume). At Site 895, most samples have values that fall between 10° and 60°, although several samples from Hole 895D have low or negative inclination values. The wide scattering for Hole 895D samples (-59° to +59°) suggests that Hole 895D penetrated large boulders or blocks (roughly 10–20 m in scale) that experienced different amounts of rotation.

The expected magnetic inclination for the latitude of Hess Deep (2°N) is very near zero. Despite the large scatter in I_{stable} values for Hole 895D, most stable inclination values from Sites 894 and 895 fall within a fairly narrow range, but have I_{stable} values that are substantially higher than expected (40° and 36°, respectively). This suggests that the two blocks drilled at Sites 894 and 895 experienced a similar amount of tectonic rotation about a horizontal axis subsequent to acquisition of remanent magnetization. The oxide petrography and magnetic properties measurements indicate the remanent magnetization of the gabbros (Hole 894G samples) and harzburgites and dunites (Holes 895D and 895E) is carried by magnetite formed by alteration of silicate minerals (olivine and pyroxene for the gabbros and olivine for the peridotites). This suggests that the tectonic rotation occurred after the alteration events, which could be related either to ridge processes or to the opening of Hess Deep.

Physical Properties

The rocks drilled at both Sites 894 and 895 provide an opportunity to better constrain the physical properties of the lower crust and shallow mantle generated at a fast-spreading ridge. The contrasting lithologies between the two sites result in variable physical properties.

The average bulk density of the Site 894 samples is 2.92 ± 0.09 g/cm³ (Fig. 5), with the lowest densities corresponding to the most altered samples. The gabbroic samples from Site 895 have a slightly lower average density (2.81 ± 0.07 g/cm³), which is attributed to a more pervasive alteration. The density of peridotites highly contrasts with the gabbros, due to extensive serpentinization (Fig. 5). The mean bulk density value for the harzburgites is 2.66 g/cm³ \pm 0.10 g/cm³, whereas the dunites, generally more serpentinized, have a mean of 2.54 g/cm³ \pm 0.03 g/cm³. At both sites, densities show an inverse correlation with porosities.

Compressional P -wave velocities were measured on both vertical and horizontal minicores with respect to the drilled core. At Site 894, the mean horizontal velocity measured in the gabbros is 6587 m/s \pm 564 m/s. The ultramafic rocks from Site 895 have much lower velocities; the mean value for harzburgite is 5558 m/s \pm 535 m/s, and for dunite is 4946 m/s \pm 298 m/s. The low mean values for both the harzburgite and dunite reflect the high degree of serpentinization and correlate with low densities and high porosities. Velocities measured in several vertical and horizontal samples of the gabbros from Site 894 do not show any significant anisotropy. In contrast, adjacent perpendicular minicores from Site 895 show a consistent trend of lower vertical velocities with respect to their corresponding horizontal pair. At this point, we can only suggest that these variations might be caused either by the subhorizontal to horizontal preferred mi-

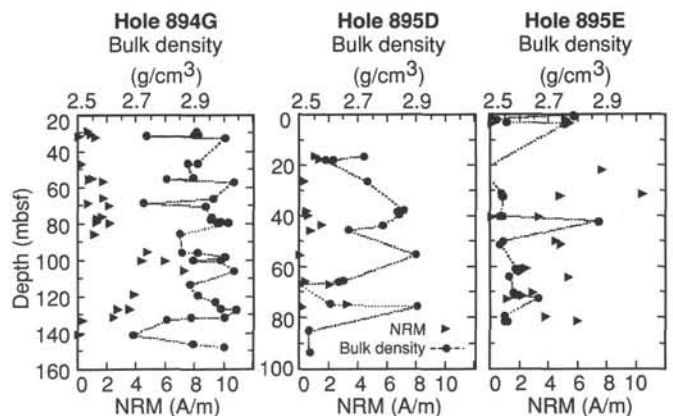


Figure 5. Plot of NRM (triangles) and density (circles) for Holes 894G, 895D, and 895E.

crocrack orientation or by preferred mineral orientation within the observed foliation and serpentine fabric.

Conclusions

The plutonic rocks recovered at Site 894 represent a sequence of high-level gabbros that may have crystallized along the margin of a magma chamber downward from evolving tholeiitic magma. Stratigraphically, Site 894 appears to lie between the plutonics exposed ~20 km northeast of Site 894 along the northern rift valley wall and those that crop out along the slope south of the intrarift ridge. The northern scarp plutonics crop out immediately below the sheeted dike complex and include "gabbros of basaltic composition" and gabbro cumulates. The basaltic composition of the shallowest gabbros does not show the geochemical effect of primocryst concentration and may represent the base of the sheeted dike complex (Natland, 1990). The gabbro cumulates, which occur about 200 m below the "gabbros of basaltic composition," include gabbros, gabbroonorites, and norites with <1% primary interstitial oxides. Significantly, none of these rocks contain olivine. The plutonic rocks that crop out south of the crest of the intrarift ridge vary in lithologic type downslope from gabbros to primitive olivine gabbros, troctolites, dunites, and tectonized serpentinites (Francheteau et al., 1990; Hekinian et al., 1993), and are more primitive than most of the Site 894 plutonics (Hekinian et al., 1993).

The plutonic rocks recovered at Site 894 are comparable to the olivine-poor gabbros, gabbroonorites, and disseminated-oxide gabbros from Hole 735B. However, the Site 894 section lacks the fairly primitive troctolites and olivine gabbros as well as the high-SiO₂ trondhjemite or felsic dikelets that are associated with Fe-Ti oxide gabbros at Hole 735B. The full range of rocks in this 500-m hole at 735B actually well matches the range found in all localities within Hess Deep. Only the truly primitive Hess Deep olivine gabbros and troctolites sampled by *Nautile* have no generic equivalents at Hole 735B.

The most significant difference between the plutonic rocks recovered at Site 894 and those at Hole 735B is the absence of ductile deformation in the Hess Deep gabbroic rocks. At Site 894, there are examples of magmatic foliation, but these were evidently acquired within a significantly molten crystal mush, and do not represent large-scale processes.

Metamorphism of the Site 894 plutonics differs in many respects from the gabbro exposures elsewhere in the Hess Deep region. The plutonic rocks from the northern scarp are altered to lower amphibolite to greenschist facies mineral assemblages; however, the intensity of metamorphism is typically much less than that observed at Site 894 (Gillis and Natland, 1990). Static alteration is typically concentrated along microfractures and is similar to the earliest veins documented at Site 894. The northern scarp gabbros lack the intermediate- to late-stage veins that are dominant at Site 894. Moreover, the northern scarp gabbros lack cataclastic deformation. In contrast to the northern scarp and Site 894, many of the plutonic rocks recovered along the slope south of the crest of the intrarift ridge are pervasively amphibolitized or rodingitized (Hekinian et al., 1993). As at Site 894, cataclastically deformed rocks are common.

The differences in the intensity and style of alteration between the Site 894, northern scarp, and southern slope gabbroic rocks may be related to a variety of processes. If it is assumed that most of the static alteration is related to early hydrothermal processes at or near the EPR axis, the observed variation in the intensity of alteration may indicate that these exposures of plutonic rocks formed along different parts of a ridge segment. The high density of the intermediate- to late-stage prehnite/chlorite veins at Site 894, which are not prevalent along the northern scarp, may be related to opening of the Cocos-Nazca ridge. Moreover, the cataclasites from Site 894 and the southern slope are probably associated with normal faulting associated with extension during Cocos-Nazca rifting.

The harzburgites recovered at Site 895 are typical of residual mantle peridotites with porphyroclastic textures, and contain a min-

eral assemblage consisting largely of olivine and lesser orthopyroxene with minor amounts of clinopyroxene and spinel. Clinopyroxene is usually low in abundance (less than 1%), though locally it may amount to 3% of the peridotite. This assemblage suggests that harzburgite from Hess Deep is refractory and represents melting of the Pacific mantle to a clinopyroxene-out or nearly clinopyroxene-out residue. The large suites of abyssal peridotites dredged from fracture zones and rift valley walls from the Atlantic and Indian oceans contain 3.5% diopside on average (Dick, 1989). By comparison, the rocks from Hess Deep are moderately to highly depleted. The presence of refractory peridotite residue suggests that relative to the mantle beneath other regions of the global ridge system, either higher degrees of partial melting with effective melt extraction prevailed or the mantle here was initially more refractory.

The abundance of dunites at Site 895 is striking. The relatively common occurrence of dunite associated with refractory harzburgite may be characteristic of the Hess Deep upper mantle. The dunites may alternatively be the products of melt/mantle rock reaction or simple cumulus products of melt crystallization. Melt injection is consistent with the appearance of gabbroic and troctolitic rocks within dunite-dominant intervals of the Site 895 cores, particularly those from Hole 895E and the lower part of Hole 895D. Some of the olivine in the olivine gabbros may be modified xenocrysts and xenoliths of mantle olivine.

In the Hess Deep intrarift ridge suite, the relative abundance of dunite, and its association with gabbroic rocks, suggests that the drilled sections of Site 895 are close to the mantle-crust boundary as recognized in ophiolite complexes such as the Semail ophiolite. The varying proportions of harzburgites, dunites, and gabbroic rocks in the different holes suggest a laterally heterogeneous mantle beneath the East Pacific Rise, which was associated with nonuniform distribution of flow of melt out of the mantle.

The propagation of the Cocos-Nazca ridge into EPR-generated crust exposed at Hess Deep may have left magmatic, metamorphic, and structural imprints on the Leg 147 samples. Preliminary structural reconstructions, using paleomagnetic data, suggest that the orientation of late fractures and cataclastic deformation in the gabbros are parallel to the Cocos-Nazca propagator. At what time and to what extent this deformation influenced the crust exposed at Hess Deep is not well constrained, but this is of major importance for understanding the timing of seawater penetration into the crust and the serpentinization process.

The results of Leg 147 may be used to understand the mechanism responsible for the uplift of the intrarift ridge. Magnetic inclinations are consistent between Sites 894 and 895, suggesting the same amount of block rotation at both sites, after alteration of both gabbros and peridotites. One of the two models proposed by Francheteau et al. (1990) to explain the distribution of lithologies at Hess Deep involves serpentinite diapirism. Although the bulk density of the serpentinitized peridotites from Site 895 is significantly lower than that of the gabbros, most of the serpentinization that affected the peridotites occurred under static conditions. Therefore, there is no direct evidence from Site 895 to support the diapiric model.

REFERENCES*

- Bird, D.K., Rogers, R.D., and Manning, C.E., 1986. Mineralized fracture systems of the Skaergaard intrusion. *Medd. Groenl.: Geosci.*, 16:68.
 Bloomer, S.H., Meyer, P.S., Dick, H.J.B., Ozawa, K., and Natland, J.H., 1991. Textural and mineralogical variations in gabbroic rocks from Hole 735B. In Von Herzen, R.P., Robinson, P.T., et al., *Proc. ODP, Sci. Results*, 118: College Station, TX (Ocean Drilling Program), 21-40.
 Blum, N., 1991. Structure and composition of oceanic crust and upper mantle exposed in Hess Deep of the Galapagos Microplate (Equatorial East Pacific) [Ph.D. dissert.]. Univ. Karlsruhe, Germany.

* Abbreviations for names of organizations and publication titles in ODP reference lists follow the style given in *Chemical Abstracts Service Source Index* (published by American Chemical Society).

- Cannat, M., Mével, C., and Stakes, D., 1991. Normal ductile shear zones at an oceanic spreading ridge: tectonic evolution of Site 735 gabbros (southwest Indian Ocean). In Von Herzen, R.P., Robinson, P.T., et al., *Proc. ODP, Sci. Results*, 118: College Station, TX (Ocean Drilling Program), 415–430.
- Casey, J.F., Rowley, M., Xia, C., and Kurz, M., 1990. Lower crustal rheology, strain localization, low-angle seismic reflectors and deep hydrothermal penetration in near-ridge environments. *Eos*, 71:629.
- Crane, K., 1985. The spacing of rift axis highs: dependence upon diapiric processes in the underlying asthenosphere. *Earth Planet. Sci. Lett.*, 72:405–414.
- Detrick, R.S., Buhl, P., Vera, E., Mutter, J., Orcutt, J., Madsen, J., and Brocher, T., 1987. Multi-channel seismic imaging of a crustal magma chamber along the East Pacific Rise. *Nature*, 326:35–41.
- Dick, H.J.B., 1989. Abyssal peridotites, very slow spreading ridges and ocean ridge magmatism. In Saunders, A.D., and Norry, M.J. (Eds.), *Magmatism in the Ocean Basins*. Geol. Soc. Spec. Publ. London, 42:71–105.
- Dick, H.J.B., Meyer, P.S., Bloomer, S., Kirby, S., Stakes, D., and Mawer, C., 1991. Lithostratigraphic evolution of an in-situ section of oceanic Layer 3. In Von Herzen, R.P., Robinson, P.T., et al., *Proc. ODP, Sci. Results*, 118: College Station, TX (Ocean Drilling Program), 439–540.
- Francheteau, J., Armijo, R., Cheminée, J.L., Hekinian, R., Lonsdale, P., and Blum, N., 1990. 1 Ma East Pacific Rise oceanic crust and uppermost mantle exposed by rifting in Hess Deep (equatorial Pacific Ocean). *Earth Planet. Sci. Lett.*, 101:281–295.
- Francheteau, J., Armijo, R., Cheminée, J.L., Hekinian, R., Lonsdale, P., and Blum, N., 1992. Dike complex of the East Pacific Rise exposed in the walls of Hess Deep and the structure of the upper oceanic crust. *Earth Planet. Sci. Lett.*, 111:109–121.
- Gillis, K., and Natland, J., 1990. Patterns of alteration in crustal sections exposed at the Hess Deep, Equatorial Pacific. *Eos*, 71:1697.
- Girardeau, J., and Francheteau, J., 1993. Plagioclase-wehrlites and peridotites on the East Pacific Rise (Hess Deep) and the Mid-Atlantic Ridge (DSDP Site 339): evidence for magma percolation in the oceanic upper mantle. *Earth Planet. Sci. Lett.*, 115:137–149.
- Hekinian, R., Bideau, D., Francheteau, J., Lonsdale, P., and Blum, N., 1993. Petrology of the East Pacific Rise crust and upper mantle exposed in the Hess Deep (eastern equatorial Pacific). *J. Geophys. Res.*, 98:8069–8094.
- Hekinian, R., Thompson, G., and Bideau, D., 1989. Axial and off-axis heterogeneity of basaltic rocks from the East Pacific Rise at 12°35'N–12°51'N and 11°26'N–11°30'N. *J. Geophys. Res.*, 94:17437–17463.
- Huang, P.Y., and Solomon, S.C., 1988. Centroid depths of mid-ocean ridge earthquakes: dependence on spreading rate. *J. Geophys. Res.*, 93:13445–13477.
- Karson, J., Thompson, G., Humphris, S.E., Edmond, J., Bryan, W.B., Brown, J.R., Winters, A.T., Pockalny, R.A., Casey, J., Campbell, A.C., Klinkhammer, G.P., Palmer, M.R., Kinzler, R.J., and Sulanowska, M.M., 1987. Along-axis variations in seafloor spreading in the MARK area. *Nature*, 328:681–685.
- Karson, J.A., Hurst, S.D., and Lonsdale, P.F., 1992. Tectonic rotations of dikes in fast-spread oceanic crust exposed near Hess Deep. *Geology*, 20:685–688.
- Kent, G.M., Harding, A.J., and Orcutt, J.A., 1990. Evidence for a smaller magma chamber beneath the East Pacific Rise at 9°30'N. *Nature*, 344:650–653.
- Langmuir, C.H., Bender, J.F., and Batiza, R., 1986. Petrologic and tectonic segmentation of the East Pacific Rise, 5°30'–14°30'. *Nature*, 322:422–429.
- Lin, J., Purdy, G.M., Schouten, H., Sempéré, J.-C., and Zervas, C., 1990. Evidence from gravity data for focussed magmatic accretion along the Mid-Atlantic Ridge. *Nature*, 344:627–632.
- Lonsdale, P., 1988. Structural pattern of the Galapagos microplate and evolution of the Galapagos triple junction. *J. Geophys. Res.*, 93:13551–13574.
- MacDonald, K., 1987. Tectonic evolution of ridge-axis discontinuities by the meeting, linking or self-decapitation of neighboring ridge sediments. *Geology*, 15:993–997.
- McCarthy, J., Mutter, J.C., Morton, J.L., Sleep, N.H., and Thompson, G.T., 1988. Relic magma chamber structures preserved within the Mesozoic North Atlantic crust? *Geol. Soc. Am. Bull.*, 100:1423–1436.
- Mével, C., and Cannat, M., 1991. Lithospheric stretching and hydrothermal processes in oceanic gabbros from slow-spreading ridges. In Peters, T., Nicolas, A., and Coleman, R.G. (Eds.), *Ophiolite Genesis and Evolution of the Oceanic Lithosphere*: Dordrecht (Kluwer), 293–312.
- Murdmaa, I.O., and Rozanova, T.V., 1976. Hess Deep bottom sediments. In *Geological–Geophysical Researches in the Southeastern Part of the Pacific Ocean*: Moscow (Nauka), 252–260. (in Russian)
- Natland, J., 1990. High level gabbros of the East Pacific Rise sampled by submersible at fault exposure in Hess Deep, Equatorial Pacific. *Eos*, 71:1647.
- Nehlig, P., and Juteau, T., 1988. Flow porosities, permeabilities and preliminary data on fluid inclusions and fossil thermal gradients in the crustal sequence of the Sumail ophiolite (Oman). *Tectonophysics*, 151:199–221.
- Neprochnov, Y.P., Sedov, V.V., Semenov, G.A., Yelnikov, I.N., and Filaktov, V.D., 1980. The crustal structure and seismicity of the Hess Basin area in the Pacific Ocean. *Oceanology*, 20:317–322.
- Nicolas, A., 1989. *Structure of Ophiolites and Dynamics of the Oceanic Lithosphere*: Dordrecht (Kluwer).
- Pallister, J.S., and Hopson, C.A., 1981. Samail ophiolite plutonic sequence: field relations, phase variation, cryptic variation and layering, and a model of a spreading ridge magma chamber. *J. Geophys. Res.*, 86:2593–2644.
- Purdy, G.M., and Detrick, R.S., 1986. Crustal structure of the Mid-Atlantic Ridge at 23°N from seismic refraction studies. *J. Geophys. Res.*, 91:3739–3762.
- Rudnick, G.B., 1976. Magmatic and metamorphic rocks of the Hess basin. In *Geologic Studies in the Southeastern Part of the Pacific Ocean*. Ocean. Stud., 29:44–56.
- Schmitz, W., Singer, A., Bäcker, H., and Stoffers, P., 1982. Hydrothermal serpentine in a Hess Deep sediment core. *Mar. Geol.*, 46:M17–M26.
- Sempéré, J.-C., Purdy, G.M., and Schouten, H., 1990. Segmentation of the Mid-Atlantic Ridge between 24°N and 30°40'N. *Nature*, 344:427–431.
- Sinton, J.M. and Detrick, R.S., 1992. Mid-ocean ridge magma chambers. *J. Geophys. Res.*, 97:197–216.
- Stakes, D., Mével, C., Cannat, M., and Chaput, T., 1991. Metamorphic stratigraphy of Hole 735B. In Von Herzen, R.P., Robinson, P.T., et al., *Proc. ODP, Sci. Results*, 118: College Station, TX (Ocean Drilling Program), 153–180.
- Toomey, D.R., Solomon, S.C., Purdy, G.M., and Murray, M.H., 1985. Microearthquakes beneath the median valley of the Mid-Atlantic ridge near 23°N: hypocenters and focal mechanisms. *J. Geophys. Res.*, 90:5443–5458.
- Whitehead, J.A., Dick, H.J.B., and Shouten, H., 1984. A mechanism for magmatic accretion under spreading centers. *Nature*, 312:146–148.
- Wiggins, S., Canuteson, E.L., Dorman, L., Hildebrand, J., Sauter, A., and Schreiner, A.E., 1992. Crustal structure at the Hess Deep: seismic studies show high surficial velocity and density on the intrarift ridge. *Eos*, 76:356.
- Zonenshain, L.P., Kogan, L.I., Savostin, L.A., Golmstock, A.J., and Gorodnitskii, A.M., 1980. Tectonics, crustal structure and evolution of the Galapagos Triple Junction. *Mar. Geol.*, 37:209–230.

Ms 1471R-101